



# Phase wetting detection and water layer thickness characterization in two-phase oil-water flow using high frequency impedance measurements



L.D. Paolinelli<sup>\*</sup>, J. Yao, A. Rashedi

*Institute for Corrosion and Multiphase Technology, Department of Chemical & Biomolecular Engineering, Ohio University, 342 W. State Street, Athens, OH 45701, USA*

## ARTICLE INFO

### Keywords:

Phase wetting  
Multiphase flow  
High frequency impedance  
Conductance  
Water layer  
Corrosion

## ABSTRACT

Two-phase oil-water pipe flow is common in oil production. When transported water contacts pipeline walls, a phenomenon known as water wetting, severe internal corrosion can occur. Water wetting can be avoided by entrainment of the water phase into the oil phase. Consequently, it is of great interest to understand operating conditions where this happens. Various experimental works have been performed to study water wetting in oil-water pipe flow. In general, two-electrode DC conductance measurements have been used to detect water wetting. Despite its implementation, application of this analytical setup is not straightforward; it requires extensive calibration due to the effect of the electrochemical reactions occurring at electrode surfaces. Moreover, reliable conductance measurements of the water phase are unobtainable. Proper estimation of important geometric characteristics such as the thickness of water layers is not possible, either. In this work, high frequency impedance measurements on a flush mounted two-electrode concentric probe are used in order to detect phase wetting regimes in large-scale oil-water pipe flow, as well as to determine the water layer thickness associated with water wetting. Formulae that correlate the resistance of sensed water layers with their actual thickness are described and validated. Excellent results in terms of phase wetting detection are obtained and dynamic characterization of the water layer thickness is also enabled.

## 1. Introduction

Two-phase flow of liquid hydrocarbons and water is commonly found in pipelines associated with oil production facilities. In such cases, contact between water and internal pipe wall can be a great concern, since it can lead to serious corrosion problems when materials such as carbon steel are used (Kermani and Morshed, 2003; Pots et al., 2006; Smith and Joosten, 2006). This scenario is called water wetting (Cai et al., 2012; Pots et al., 2006). It is considered that under regular production conditions the hydrocarbon phase is not corrosive (Cai et al., 2012; Lotz et al., 1991). Therefore, if the water phase is disrupted and entrained into the turbulent oil phase flow, water wetting and internal corrosion risks can be avoided. Laboratory tests to determine phase wetting regimes in two-phase hydrocarbon-water pipe flow have been of great interest in corrosion engineering. In particular, knowing which operating conditions to select can minimize the risk of internal corrosion (Ayello et al., 2008; Cai et al., 2012; Kee et al., 2016; Pots et al., 2006). In general, these experimental efforts have been conducted using flow loops instrumented with flush-mounted conductance probes (Cai et al., 2012; Kee et al., 2016) and/or impedance probes (Valle, 2000).

Ayello et al. (2008), Cai et al. (2012), and Kee et al. (2016). used arrays of staggered small diameter two-electrode DC conductance probes, flush-mounted in a carbon steel pipe, to capture phase wetting behavior in two-phase oil-water flow. These two-electrode concentric conductance probes are connected in series with a 1 M $\Omega$  resistor and receive a constant voltage excitation when operated. As water is significantly more conductive than oil or air, particularly when it contains dissolved salts, it is detected when it covers the probe contacts by comparing the voltage at the node located between the probe and the 1 M $\Omega$  resistor with a calibrated voltage reference. One advantage of this instrumentation setup is that a large number of staggered probes are used around and along the circumference of the pipe. This helps to detect the water phase in case it “snakes” around individual probes, which could lead to false readings. Moreover, this setup has proved to be very convenient when assessing phase wetting in three-phase oil-water-gas flow, in which water can be present not only at the pipe bottom but also all around the pipe circumference (Kee et al., 2015). However, since the obtained response is “on-off” type, it is not possible to know the thickness of the water layer in contact with the probe surface. For example, thin aqueous residues left on top of the probes give similar readings to considerably thicker segregated

<sup>\*</sup> Corresponding author.

E-mail address: [paolinel@ohio.edu](mailto:paolinel@ohio.edu) (L.D. Paolinelli).

water layers produced by consistent water dropout, leading to ambiguous results.

Valle (2000) used AC measurements for water wetting characterization in two-phase oil-water flow. The employed setup was flush-mounted parallel plate two-electrode probes with 1 kHz frequency excitation. Despite the use of AC, the author required calibration to interpret the probe response and only obtained information relating to the presence or absence of the water phase on the pipe surface. This is unsurprising since, in general, frequencies higher than 1 kHz are needed to avoid the effect of electrochemical double layer on the measured impedance (Asali et al., 1985; Coney, 1973).

Given all the experimental work performed so far on water wetting, there is no information in the literature about the thickness of water layers in contact with the pipe wall. However, this is an important parameter that can be used to validate or develop hydrodynamic models, as well as to estimate the internal corrosion rate of the pipe. For example, mass transfer of corrosive species to the pipe surface is affected by the velocity of the water layer (Nešić, 2007), which is proportional to its thickness. Moreover, very thin water layers can flow so slowly and be so poorly replenished by the dispersed water droplets that they get rapidly saturated with dissolved metallic ions (e.g., ferrous ions) from the occurring corrosion processes. Under this circumstance, corrosion products can then precipitate forming a protective barrier which reduces corrosion rate (Kermani and Morshed, 2003; Nešić, 2007).

The use of flush mounted AC conductance probes has been theoretically treated and reported for the measurement of liquid film thickness in two-phase flow (Coney, 1973). Based on this, other researchers (Asali et al., 1985; Andreussi et al., 1988); devised flush mounted two parallel ring electrodes to sense liquid holdup and thickness of annular liquid films in liquid-gas pipe flow using high frequency impedance measurements. Due to the successful use of this setup, additional analytical solutions were further developed for the measurement of conductance of annular liquid films using parallel ring electrodes in gas-liquid flow with and without packed beds (Tsochatzidis et al., 1992). Several recent studies have successfully used the parallel ring conductance method with high frequency AC excitation to measure water holdup in stratified oil-water pipe flow (Tan et al., 2013, 2015; Wu et al., 2015; Zhai et al., 2012, 2015). Although the two parallel ring electrode setup is fairly accurate to sense liquid holdup in stratified flow and liquid film thickness in annular flow, it cannot resolve which location of the pipe circumference the liquid layer wets. Therefore, this design of probe does not offer much advantage for phase wetting studies.

Other geometrical configurations of conductance probes as parallel wires can produce reliable local measurements of liquid holdup or liquid film thickness when used with high frequency AC excitation as reported for gas-liquid flow (Andreussi et al., 2016; Brown et al., 1978) and liquid-liquid pipe flow (Zhai et al., 2015). Nevertheless, this configuration is intrusive and can perturb the flow, which is undesirable when sensing phase wetting.

Two separated flush-mounted circular electrodes have also been used with AC to measure the local thickness of liquid layers in a pipe in static conditions and in annular liquid-gas flow (Asali et al., 1985). Good agreement was found between the conductance values measured using 100–500 kHz AC excitation and the theoretical calculations for liquid layers thicknesses ranging from 0.1 to 1 mm. Researchers later demonstrated the use of flush-mounted two-electrode concentric probes with 5 kHz AC excitation arranged around the pipe circumference to characterize local liquid film thickness in annular gas-liquid flow (Zhao et al., 2013). The electrical signal was processed using a voltage-conductance calibration curve and an expression relating conductance and liquid layer thickness obtained from numerical methods. Recent studies have involved use of flush mounted two-electrode parallel plates and concentric probes excited with AC to measure water layer velocity in oil-water pipe flow (Koguna et al., 2015). The authors mentioned the potential use of these probes to monitor *in situ* the height of flowing water layers via prior calibration of the probe. The latter may not be necessarily

needed upon proper understanding of the electrical response of the used probe and measured fluids.

The use of properly selected AC excitation can greatly help to overcome several intrinsic drawbacks of DC measurements. Conduction of electrons from the probe electrodes to the water or any other electrolyte is produced by means of oxidation and reduction of ionic species at the exposed electrode surfaces. These Faradaic electrochemical processes produce resistive (charge transfer resistance) and capacitive (double layer capacitance) effects that are proportional to the wetted area of the electrodes that, in the case of a two-electrode configuration, represent two impedances in series with the conductive and dielectric impedance of the electrolyte. When DC excitation is used, the measured resistance corresponds to the summation of the oxidation charge transfer resistance on the wetted surface of one electrode, the electrolyte resistance, and the reduction charge transfer resistance on the wetted surface of the other electrode. In general, the electrolyte resistance, which only depends on the geometry of the fluid/electrodes arrangement, can be orders of magnitude lower than the Faradaic resistances. Moreover, the Faradaic resistances also depend on the excitation potential, temperature, and type and concentration of species dissolved in the electrolyte that can be reduced or oxidized. Therefore, DC measurements in two-electrode setups rarely represent the conductive behavior of the electrolyte solely, and usually require extensive calibration since the total voltage drop will depend on the several aforementioned factors. These aspects have been thoroughly discussed decades ago (Coney, 1973), and are the reason why researchers have employed high frequency AC excitation to obtain proper conductance measurements in two-electrode probe configurations. At high enough frequencies, the impedance in series offered by the double layer capacitance becomes so low that the resistance of the water phase can be accurately measured. In this case, if the probe geometry and dimensions as well as electrolyte conductivity are known, calibration of the probe may not be needed.

It is worth stressing that most of the studies using two-electrode probes (flush mounted or not) excited with high frequency did not require calibration to interpret the electrical measurements and extract parameters relating to liquid layer thickness per the knowledge of the theoretical response of the probe (Asali et al., 1985; Brown et al., 1978; Coney, 1973; Tsochatzidis et al., 1992). For all the aforementioned reasons, the use of high frequency AC excitation in two-electrode setups is more advantageous than DC excitation when performing conductance measurements. However, AC measurements require shielded wiring and more complex electronics (e.g., high quality wave generator) than DC measurements; for example, the use of a potentiostat with an impedance unit. The need for more complex electronics, in some cases, can pose a limitation when implementing AC setups in lab and industrial facilities. Nevertheless, high quality electronics have become more available and less expensive.

In some experimental systems, less complex circuits using DC excitation can be successfully used to measure liquid layer thickness. For example, Al-Sarkhi et al. used flush-mounted two-electrode parallel plate probes arranged around the pipe circumference to measure liquid thickness in annular gas-liquid inclined flow (Al-Sarkhi et al., 2012). The authors used pulses of DC excitation and monitored the current circulating across the probes. The probe response was calibrated dynamically using a micrometer and a conductivity circuit with one lead in the flowing film and a micrometer tip being used as the second lead. The use of this DC setup nevertheless involves important drawbacks when measuring the thickness of segregated water layers in oil-water flow; particularly, when thin oil residues remain adsorbed on the probe electrodes partially covering their surfaces while a water layer flows on top. Since Faradaic resistances at the two electrodes are proportional to the fraction of their surface that is effectively water wet, the total measured resistance across the probe can be significantly altered from the calibration value corresponding to full coverage of the electrodes, leading to erroneous water layer thickness estimation. Partial coverage of metal surfaces with thin oil films is very likely to occur, favored by the presence

of surfactants dissolved in the water or the oil phase and/or organic compounds present in the oil (Ayello et al., 2013). In this respect, high frequency impedance measurements are mostly insensitive to partial coverage of the electrode surfaces when the operating frequency is properly selected.

Surprisingly, despite the great potential of local two-electrode flush mounted probes excited with high frequency AC, such setups have rarely been used to quantify liquid layer thicknesses and/or sense phase wetting in liquid-liquid flow (Riaño et al., 2015). This is probably due to the fact that most of the research efforts have focused on determining other flow characteristics such as average and local phase holdup, amongst other phenomena.

The aim of this work is to study the use of high frequency impedance measurements using a flush mounted two-electrode concentric probe design in order to detect phase wetting regimes in oil dominated oil-water flow, as well as to determine the water layer thickness in cases of water wetting. Theoretical formulations to estimate the resistance of a water layer as a function of its thickness are introduced for the used probe geometry, and results are experimentally validated. The performance of the impedance probe is tested in dynamic conditions with a large scale flow loop of 0.1 m ID in oil-water flow with different oil and water flow rates. Excellent results in terms of phase wetting detection are obtained and water layer thickness is dynamically characterized.

## 2. Materials and methods

### 2.1. Impedance probe

The impedance probe selected for this study (depicted in Fig. 1) is a standard linear polarization resistance probe commonly used for corrosion studies (Farelas et al., 2013). This choice is convenient since such probes can be easily installed in large scale flow loop test sections and positioned flush-mounted with the internal pipe wall. Specifically, the two-electrode concentric contacts are the outer stainless steel ring and the inner carbon steel ring, which are separated by an epoxy insulator. The internal radius of the outer ring ( $r_o$ ) is 12.5 mm and the external radius of the inner ring ( $r_i$ ) is 6.2 mm. The two electrodes have the same width ( $w$ ), 3 mm.

In oil-water flow water wetting studies, it is of interest to detect when water is no longer stably dispersed in oil and drops out due to the effect of gravity leading to rivulets or water layers forming at the bottom wall of the pipe. In this scenario, the impedance probe can sense the constant or alternating presence of a water film or layer covering completely or partially its contacts. The total measured impedance ( $Z_t$ ) can be defined as the impedance of the probe ( $Z_p$ ) considered in parallel with the impedances of the fluids on top of its contacts, namely, a water layer ( $Z_w$ ), an oil layer ( $Z_o$ ), or a water-in-oil mixture layer ( $Z_m$ ). The oil or the water-

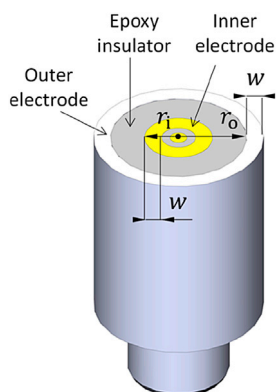


Fig. 1. Schematic of the used impedance probe. Drawing courtesy of Cody Shafer.

in-oil mixture layer present very low capacitance and very high resistance compared to the probe itself or the water layer. Therefore, when the probe is wetted by an oil or water-in-oil mixture layer, the total measured impedance is  $Z_t = Z_p$  since the impedance of the liquid is sufficiently high so that it does not affect the measurement. When a water layer is present, the total measured impedance can be expressed as:

$$Z_t = [Z_p^{-1} + Z_w^{-1}]^{-1} \quad (1)$$

Fundamentally, the probe responds as a capacitor at high and middle frequency range, thus:

$$Z_p = -(2\pi f C_p)^{-1} j \quad (2)$$

where  $f$  is the frequency of the AC excitation and  $C_p$  is the total capacitance of the probe.

In general, the impedance of a conductive water layer consists only of a real part at high frequencies (resistive behavior). Moreover, its value is usually quite low relative to the probe. In this case, equation (1) shows that the total measured impedance is only due to the presence of water ( $Z_t \cong Z_w = R_s$ ). Fig. 2 shows the Bode plot of the typical frequency response of the probe alone and with a conductive water layer on top. At mid/low frequencies, the effect of the electrochemical double layer at the electrode surfaces becomes important when water is present, adding capacitive impedance. It is clear that to avoid the effect of Faradaic impedance in this system, frequencies higher than 1 kHz should be used.

The resistive response of a very thin water layer of thickness  $h$  that covers the probe surface uniformly can be estimated as (Fried et al., 1993):

$$R_s = \frac{1}{\kappa} \frac{\ln(r_o/r_i)}{2\pi h} \quad (3)$$

where  $\kappa$  is the conductivity of the liquid.

At this point, a simple quantitative verification of the assumptions made on the contributions of the impedances of a water layer, oil layer,

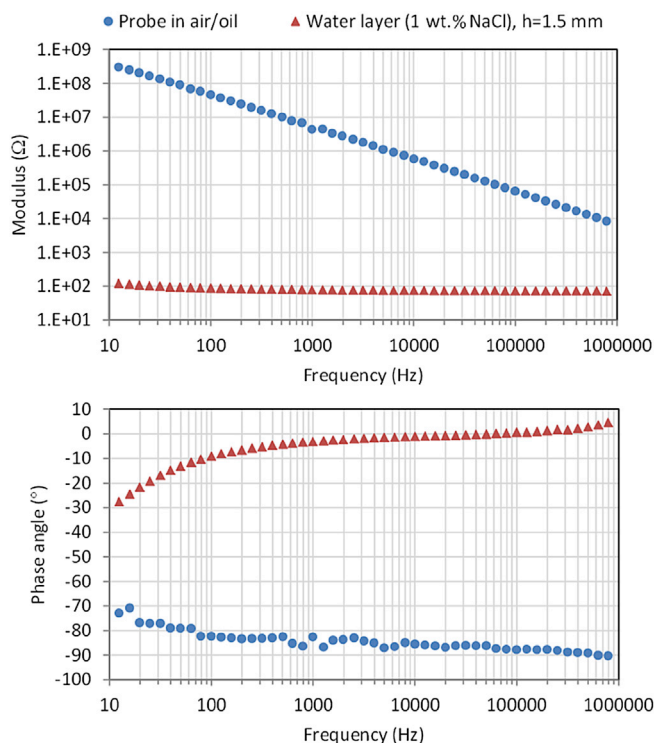


Fig. 2. Bode plot of the impedance frequency response of the probe in air or oil and with a conductive water layer on top.

and the probe on the total measured impedance can be done. For example, if a 1 mm thickness liquid layer is placed on top of the probe, its characteristic geometric constant ( $K = \ln(r_o/r_i)/2\pi h$ ) is about  $110 \text{ m}^{-1}$ . If the layer is considered as tap water (electric conductivity  $\kappa \sim 0.05 \text{ S m}^{-1}$ , and dielectric permittivity  $\epsilon \sim 700 \times 10^{-12} \text{ F m}^{-1}$ ), its resistance ( $R = K/\kappa$ ) is about  $2200 \text{ } \Omega$  and its capacitance ( $C = \epsilon/K$ ) is about  $6.3 \times 10^{-12} \text{ F}$ . On the other hand, if the layer is considered as oil (electric conductivity  $\kappa \sim 10 \times 10^{-12} \text{ S m}^{-1}$  (Judendorfer et al., 2011; Peng et al., 2014) and dielectric permittivity  $\epsilon \sim 20 \times 10^{-12} \text{ F m}^{-1}$  (Goual, 2009; Peng et al., 2014)), its resistance is about  $5.5 \times 10^{12} \text{ } \Omega$  and its capacitance is about  $1.8 \times 10^{-13} \text{ F}$ . Comparison of the resistance and capacitance values of the above considered layers with the electrical properties of the probe (capacitance of about  $2 \times 10^{-11} \text{ F}$  without wiring and resistance  $> 1 \times 10^9 \text{ } \Omega$  as inferred from Fig. 2), both the resistance of the water layer and the capacitance of the probe are the dominant contributing factors to the total measured impedance at high frequency. If a water-in-oil mixed layer is considered, its electrical properties do not vary significantly with the dispersed water volume fraction respect to the oil alone (Boyle, 1985; Hanai et al., 1962). Therefore, the conclusions relating to the quantitative analysis above still hold true.

To quantify the resistance of the larger water layer thicknesses, the theoretical solution proposed by Coney (1973) for flush mounted parallel rectangular electrodes can be adapted for the actual concentric electrode design used in this work; where the mean length of the electrodes array is  $l = \pi(r_o + r_i)$ ; and the insulator half-width is  $a = (r_o - r_i)/2$ . Therefore, the dimensionless thickness of the water layer is expressed as:

$$h^* = h/a = 2h/(r_o - r_i); \quad (4)$$

and the dimensionless half-distance between the end edge of each electrode is:

$$\lambda_i = \lambda_o = \lambda = w/a + 1 = 2w/(r_o - r_i) + 1 \quad (5)$$

Fig. 3 shows the theoretical resistance estimated using Coney's exact solution adapted to the concentric electrode geometry (solid red line) and experimental values for different water layer thicknesses (scattered circles). Exact water layer thicknesses were obtained using a parallel flat PVC piece separated by calibrated spacers on top of the probe. Water layer resistance was measured by exciting the probe with an AC voltage of 10 mV rms and frequency of 20 kHz using a Gamry REF 600<sup>®</sup> potentiostat. The aqueous electrolyte was a 1 wt% NaCl solution prepared from an analytical grade reagent and deionized water, with a measured conductivity ( $\kappa$ ) of  $1.76 \text{ S m}^{-1}$  at  $25 \text{ } ^\circ\text{C}$ .

As expected and also discussed by Coney (1973), flush-mounted probes have a depth sensing upper threshold of ca. 10 mm, as seen in Fig. 3. The adapted analytical solution agrees very well with experimental data (average difference of 10%); therefore, the probe does not require empirical calibration to relate  $h$  with the measured resistance  $R_s$ . However, since the analytical solution arises from the quotient of the solutions of two complete elliptic integrals, it presents a very complicated form when expressed as a function of the thickness of the conductive layer. Here, a simple convenient approximation of the exact solution is given as a function of the water layer thickness and the inner and outer radius of the concentric electrodes for  $\lambda_i = \lambda_o = \lambda = 2$ .

$$R_s = \frac{1}{\kappa\pi(r_o + r_i)} \left[ 1.89 + \frac{1.46}{\left(\frac{2h}{(r_o - r_i)} - 0.05\right)} \right] \quad (6)$$

equation (6) reproduces the analytical solution with no more than 5% error for dimensionless thicknesses ( $h^*$ ) equal or larger than 0.2 (dashed black line in Fig. 3). equation (3) can be used for  $h^*$  values lower than 0.2 with error below 5% (dot black line in Fig. 3).

The measured resistance values are determined with a maximum uncertainty lower than 5% in this work, and water conductivity is considered to vary no more than 5% mainly due to fluctuations in temperature (for example, from  $25 \text{ } ^\circ\text{C}$  to  $22 \text{ } ^\circ\text{C}$ ). Differentiating equation (6) with respect to the layer thickness  $h$ , it can be estimated that, for the present probe dimensions, accurate determination of the thickness of a conductive layer is limited to approximately 5 mm, where the maximum total error reaches around 20%.

For flow loop experiments, the probe surface is machined to fit the curvature of a 0.1 m ID pipe. The slight surface curvature can lead to over prediction of the conductive water layer. Coney presented an analytical expression to estimate this difference for parallel electrodes with parallel curvature axes (Coney, 1973). A maximum deviation of 5% is found for a conductive layer of 5 mm with a proportional decrease of the deviation for lower thicknesses. However, as the probe has concentric design the actual deviation is expected to be about a half of that estimated using Coney's equation.

## 2.2. Flow loop experiments

Phase wetting and water layer thickness measurements were performed in dynamic conditions in oil-water flow using a large-scale fully inclinable multiphase flow loop. A schematic layout of the flow loop is

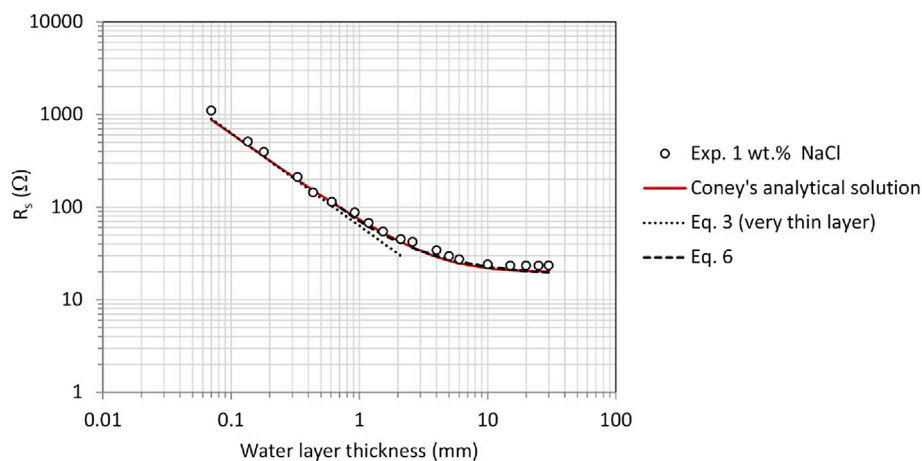


Fig. 3. Measured resistance of the water layers ( $R_s$ ) as a function of their thickness showing comparisons with analytical expressions.

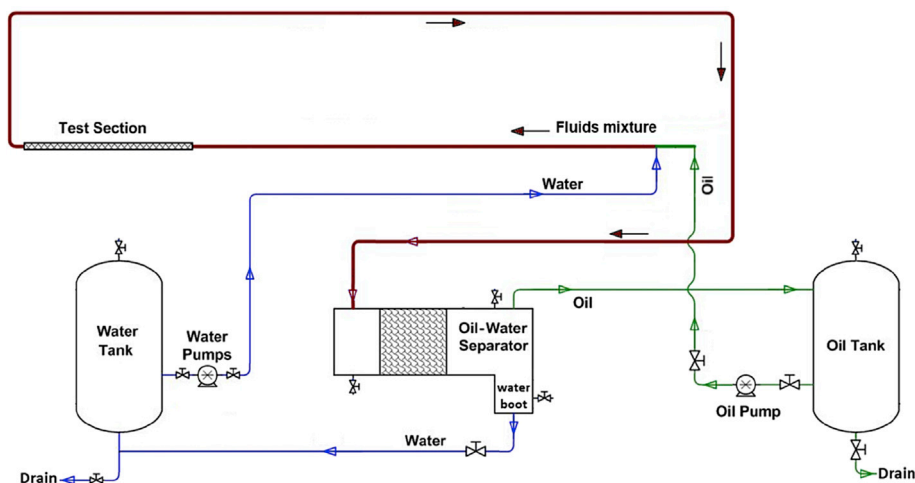


Fig. 4. Schematic layout of the 0.1 m ID flow loop used for oil-water flow tests.

shown in Fig. 4. The main part of the loop consists of a 30 m long, 0.1 m internal diameter (ID) flow line mounted on a steel rig structure. The loop consists of two parallel sections of pipes connected by a 180-degree bend. Oil and water are injected separately from the individual storage tanks (each one made of stainless steel and with a capacity of 1.2 m<sup>3</sup>) into the 0.1 m ID main line by progressive cavity pumps. Flow rates of oil and water are monitored independently by flow meters with an average accuracy of 10%. Water is injected into the main line at a T-junction through a perpendicular 0.05 m ID secondary line. The fluid mixture first flows in a stainless steel pipe (upstream leg) over a distance equivalent to approximately 140 pipe diameters allowing flow pattern and wall wetting to stabilize. The flow then enters a 1.8 m long carbon steel test section where phase wetting measurements are carried out using the impedance probe described above, flush-mounted at a distance of 16 pipe diameters downstream from the inlet of the section. A clear acrylic section is located just after the test section to allow visualization of the developed flow patterns. Upon exiting the main line, the mixture is directed to the oil-water separator described elsewhere (Cai et al., 2012). The separated oil and water streams are then returned to their respective storage tanks for further recirculation.

Before each experimental run, the internal surface of the test section was polished using a rotating flexible abrasive tool (180 grit) with deionized water as the polishing fluid. The surface was then washed with deionized water and isopropanol, then dried with a clean cloth. The roughness of the polished test section surface was indirectly measured using optical profilometry data, taken from the surface of an epoxy-mounted specimen with an area of about 5 cm<sup>2</sup> of the internal pipe wall. The measured average value in terms of arithmetic roughness ( $R_a$ ) was 1.7  $\mu\text{m}$ , with an average mean peak to valley distance ( $R_z$ ) of about 10  $\mu\text{m}$ .

Prior to introducing the impedance probe in the test section, its exposed surface was polished with a 240 grit SiC paper and deionized

water in a special device to assure the proper shape of the internal pipe curvature, and later alignment. The probe was also rinsed with deionized water and isopropanol, then dried with a clean cloth. Subsequently, the impedance probe was flush-mounted at the bottom of the carbon steel test section (Fig. 5), where water is most likely to segregate. The probe surface never intruded the oil-water flow and its height misalignment with respect to the test section surface was always lower than 0.1 mm.

Electrical measurements with the probe were with an AC voltage of 10 mV rms and frequency of 20 kHz using a Gamry REF 600<sup>®</sup> potentiostat with a computer interface. The 20 kHz frequency is high enough to avoid the interference of Faradaic impedance at the electrode surfaces on the measurements as can be inferred from Fig. 2. In the case thin oil films are partially blocking about 90% of the electrode surfaces, the capacitance due to the electrochemical double layer decreases about 1 order of magnitude, which does not practically affect impedance values measured at 20 kHz. Once the desired flow conditions were stabilized, the probe wiring was connected to the potentiostat and the impedance measurements were performed continuously for at least 1 min using a sampling rate of approximately 0.5 s.

Isopar V<sup>®</sup>, a clear saturated paraffinic hydrocarbon of density 810 kg/m<sup>3</sup> and viscosity 0.009 Pa s at 25 °C, was used as the oil phase. The water phase was the same 1 wt% NaCl solution used in the static experiments described above. The use of this highly conductive electrolyte helps preventing significant local conductivity changes when the solution comes in contact with the carbon steel test section, which easily corrodes releasing considerable amount of iron ions. The oil-water interfacial tension was measured as 0.049 N/m at 25 °C.

Flow experiments were performed in horizontal condition at room temperature ( $\sim 25$  °C) using different mixture flow velocities from 0.7 m/s to 4 m/s and water cuts from 1% to 20%. In each experimental run, the polished test section was first put in contact with oil at the highest available superficial velocity for the selected test water cut. The water was then injected and surface wetting was measured using the impedance probe. Subsequently, the oil superficial velocity was reduced to its next value maintaining the water cut, and the process was repeated until testing the lowest oil velocity. Once the experimental series was completed for the given water cut, the flow loop was drained and the test section surface was re-treated to test a different water cut.

Static wetting experiments of water-in-oil contact angles were also performed, using a goniometer, on the surface of a carbon steel specimen, prepared using the same procedure as for the test section. It was determined that the carbon steel surface behaves as hydrophilic after a few seconds, giving water-in-oil contact angles  $\theta \sim 60^\circ$  (measured from the inside of the sessile water droplet).

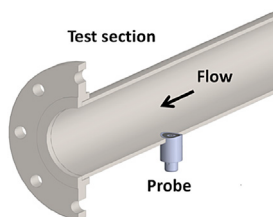


Fig. 5. Cut view of the test section with the flush-mounted probe. Drawing courtesy of Cody Shafer.

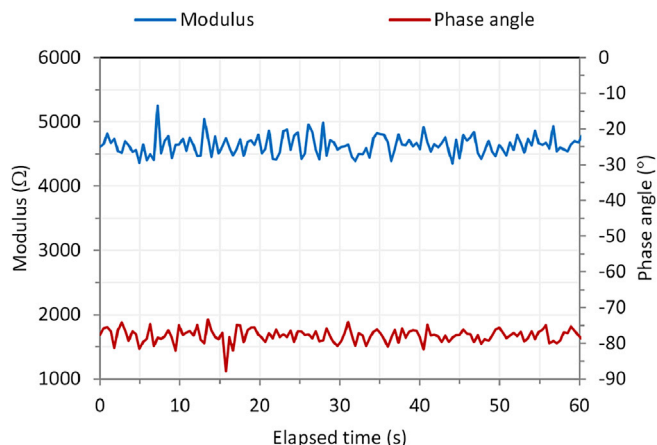


Fig. 6. Typical measured impedance at 20 kHz as a function of time for oil only flow.

### 3. Results and discussion

#### 3.1. Response of the probe to full oil wet conditions

The measured impedance of the probe and its wiring (needed for remote operation) in oil only flow was the same as in air; its modulus and phase angle are shown in Fig. 6. A time-averaged modulus of about 4650 Ω and phase angle of  $-78^\circ$  were measured at 20 kHz, with maximum deviations in time of less than 15% for both values. The measured phase angle values were somewhat higher than  $-90^\circ$  due to the slight inductive effect produced by the probe wiring. The total capacitance of the probe ( $C_p$ ) was measured as  $1.7 \times 10^{-9}$  F.

#### 3.2. Response of the probe in oil-water mixture flow

Fig. 7 show examples of the impedance response with time for oil-

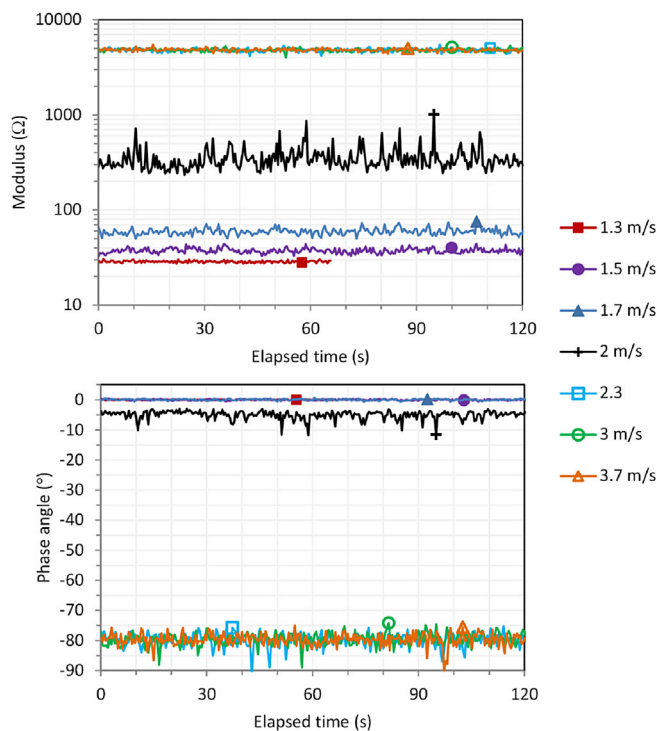


Fig. 7. Measured impedance at 20 kHz in function of time for horizontal oil-water flow with different mixture flow velocities and 3% water cut.

water flows with different mixture flow velocities and a constant water cut (WC) of 3%. Each plotted value is the average of ten different measurements separated in time by about 1 wavelength period as provided by the intrinsic settings of the potentiostat. Thus, the measurements actually capture flow events with a lower effective frequency of about 1 kHz, which is more than enough to detect the transient behavior of water layers or rivulets passing on top of the employed probe.

From Fig. 7, it is seen that for relatively large flow mixture velocities, for example 2.3 m/s or larger, the measured impedance shows capacitive behavior similar to when oil only flow is measured (Fig. 6). This indicates that all the transported water is entrained and the pipe surface is only in contact with oil. For lower mixture velocities, the measured impedance modulus decreases and the phase angle increases, indicating the presence of water wetting the pipe wall. Lower impedance modulus and a phase angle approaching zero degrees (resistive behavior) is an indication that thicker water layers were present at the lower mixture velocities.

Estimations of the thickness of the water layers detected in Fig. 7 were done using equations (1)–(4), as shown in Fig. 8. The calculated values correspond to the average thickness of the water layer flowing on top of the concentric area between the probe electrodes. Time-averaged water layer thickness values of approximately 0.13 mm, 1.2 mm, 2.5 mm and 4.3 mm were calculated for mixture velocities of 2 m/s, 1.7 m/s, 1.5 m/s and 1.3 m/s, respectively. In general, the water layers of smaller thickness display greater fluctuation with time. This is not surprising since the thinner the segregated water layer is the more unstable it becomes. This is due to the larger relative effect of mass gain *via* settling water droplets that incorporate into the film, or mass loss due to water entrained as droplets by the oil flow. It is also important to mention that water layer thickness values of the order of 0.1 mm can be somewhat biased due to the intrinsic height misalignment between the probe and the test section surface. Local flow disturbances may affect the dimensional stability of water layers as thin as those measured at a mixture velocity of 2 m/s. It is also noteworthy that the measured impedance signal can be processed instantaneously after it is obtained. This allows characterization of water layer thicknesses not only *in situ* but also in terms of how they evolve in real time. The smallest detectable water layer thickness depends on the intrinsic impedance of the probe, the conductivity of the water, and the noise level of the measured electrical signal (inherent to the quality of the electronic measurement device and wiring). For the present setup, the detection threshold is about 0.08 mm (indicated with a dashed black line in Fig. 8 for the 2.3 m/s, 3 m/s and 3.7 m/s mixture velocity series), which corresponds to the lowest fluctuating value of impedance measured in the absence of water. It is worth mentioning that the minimum detectable water layer thickness can be reduced regardless of the intrinsic electrical noise of the measurement by increasing either the water conductivity or the probe impedance (lower capacitance), which

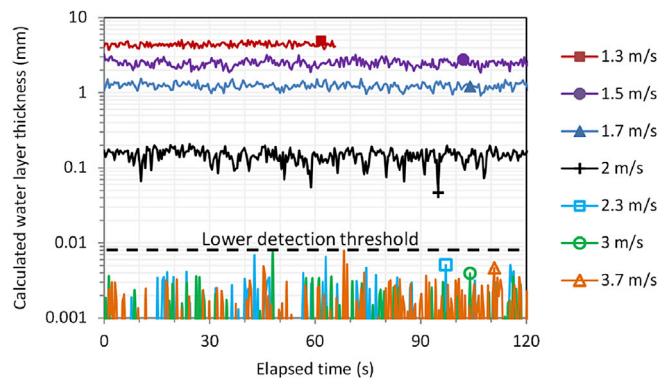


Fig. 8. Calculated water layer thickness in function of time for horizontal oil-water flows with different mixture velocities and 3% water cut.

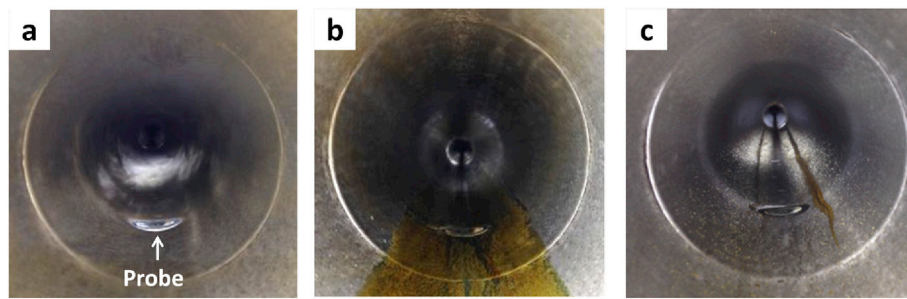


Fig. 9. Internal surface of the carbon steel test section. a) Polished fresh surface; b) After 30 min of horizontal oil-water flow with 1.7 m/s mixture velocity and 3% water cut; c) After 30 min of horizontal oil-water flow with 3.7 m/s mixture velocity and 3% water cut.

is a parameter that can be engineered jointly with the electrodes geometry to optimize the useful measurement range of the probe.

In order to corroborate the ability of the impedance measurements to sense water or oil wetting, experiments with constant flow characteristics were run and subsequent visual internal inspections of the test section performed. Each experiment started with a freshly polished surface exposed to a consistent oil-water flow regime with certain characteristics (e.g., mixture velocity of 1.7 m/s and 3% water cut) for 30 min. The water supply was then shut off and oil solely circulated for several minutes. This flow was subsequently stopped and the flow loop drained and disassembled, allowing internal inspection of the test section. Fig. 9 shows some pictures of the internal surface of the carbon steel pipe section after the tests. For the 1.7 m/s mixture velocity (Fig. 9b), evidence of a well-developed water path at the pipe bottom is clearly observed due to the presence of a corrosion product, which was absent in the areas of the pipe wall that remained oil wet. In the case of the 3.7 m/s mixture velocity (Fig. 9c), the test section surfaces did not show visible evidence of a water path intercepting the impedance probe location. Moreover, only traces of two minor water trails were found at the sides near the pipe bottom. These did not extend along the entire test section length and could have been produced by small flow disruptions produced by slight protrusions of the gasket at the flange joint upstream of the test section. Visual inspection tests proved to be in line with the impedance probe measurements regarding the presence or absence of segregated

water layers in all test cases.

Fig. 10 shows the map of phase-wetting regime built using the results obtained from the impedance probe. The map shows areas with no data at the upper right corner due to the limitation of the flow rig to deliver larger water flow rates. The plotted phase-wetting regimes are based on the results of at least 2 independent experimental runs and characterized as “full oil wet” (scattered red circles), where only oil was detected, or water wet where water was detected with different layer thicknesses; the data is arranged in ranges to illustrate their variation with flow conditions (e.g., scattered hollow green triangles indicate average water layer thicknesses between 0.1 mm and 0.5 mm). The time-averaged water layer thicknesses were calculated from the impedance data via equations (1)–(3) and (6). In general, the larger the water cut, the higher mixture velocity required to avoid water separating from a dispersed condition and generating streams or layers at the pipe bottom. For example, full oil wet to water wet transition happens at mixture velocities of about 1.7 m/s and 2 m/s for water cuts of 1% and 5%, respectively. Moreover, full oil wet regime is not observed even at mixture velocities as large as 3 m/s for water cuts larger than 5%. Instead, very thin water layers (<0.5 mm) are detected at the pipe bottom. This behavior may be related to hydrophilic nature of the surface of the carbon steel test section. Even in very turbulent flow conditions, where hydrodynamic dispersive forces of the continuous phase are significant, some dispersed water droplets will tend

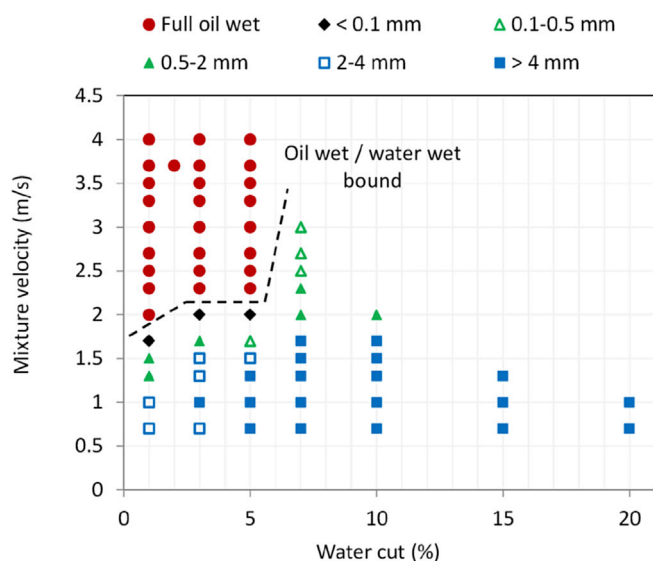


Fig. 10. Map of phase-wetting regime and time-averaged water layer thickness at the pipe bottom in horizontal oil-water flow in carbon steel pipe (0.1 m ID), obtained using the impedance probe.

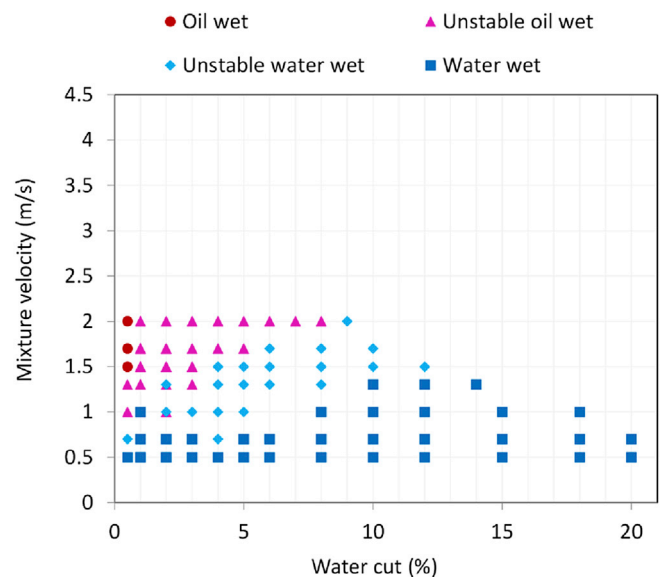


Fig. 11. Surface wetting map for horizontal oil-water flow in carbon steel pipe (0.1 m ID) from (Kee et al., 2016), obtained using flush-mounted DC probes. Oil density: 823 kg/m<sup>3</sup>, oil viscosity: 0.0027 Pa s, oil-water interfacial tension: 0.0405 N/m; water phase: 1 wt % NaCl solution.

to hit the bottom pipe wall due to the gravity action. These droplet-wall collisions are not much frequent at low droplet concentrations, but at higher droplet concentrations can occur at significant rates. Colliding water droplets are prone to stick onto the hydrophilic carbon steel surface subsequently forming thin water layers that do not grow much in thickness due to the shearing action of the continuous phase flow. Hydrophobic internal pipe walls (e.g., PVC pipes) might not show the formation of thin water layers at relatively high oil velocities and moderate water volume fractions since colliding droplets are less prone to stick onto the pipe surface.

The existence of water layers on the pipe bottom at relatively high mixture velocities (e.g., 2 m/s) and low water cuts (e.g., 1%) have also been reported by Kee et al. (Kee et al.), in similar flow experiments performed with model oil and water in carbon steel pipe using flush-mounted DC probes. Although the authors could not quantify the thickness of the occurring water layers, intermittent presence of water was detected at small areas of the bottom pipe wall, as seen in Fig. 11 as “Unstable oil wet” regime (scattered purple triangles). It is interesting to note that full oil wet (“Oil wet” regime, scattered red circles) is not achieved at the maximum tested mixture velocity of 2 m/s even for water cuts as low as 1%. This is in line with the results obtained with the high frequency (HF) impedance probe, where full oil wet occurs only at mixture velocities about or larger than 2 m/s (Fig. 10). It is also noteworthy that the slope of the transition boundary between “Unstable oil wet” and “Unstable water wet” (larger areas of the pipe bottom wall are intermittently wetted by water) regimes measured by Kee et al (Fig. 11), is similar to the slope of the gradient of water layer thickness shown in Fig. 10 (e.g., the boundary between water layer thicknesses lower and larger than 2 mm). This is not surprising since segregated water layers of larger thicknesses develop more stable in time (as shown in Fig. 8); and thus, tend to wet the pipe wall more stably.

Regarding the performance of the used HF impedance probe, it is noteworthy that when the measured amounts of water are very small (water layer thickness of the order of about 0.1 mm or lower), water is more likely to wet as tiny rivulets instead of a thin film covering the whole probe surface. Accurate characterization of water layer thickness is only possible when the impedance probe surface gets completely covered by the conductive layer. Incomplete coverage can lead to underestimation of the real layer thickness. This problem can be easily solved using a probe of smaller dimensions, but at the expense of losing depth measurement range (Coney, 1973). Arrangements of flush-mounted probes distributed along the circumference of a pipe can also be used to study phase wetting in conditions in which water can be transported to the side or top walls of the pipe (e.g., in three-phase oil-water-gas flow). Although the accuracy of water layer thickness characterization using HF impedance measurements on the flush mounted probe and signal processing based on the theoretical probe response has only been corroborated in static conditions (section 2.1), there is no reason other than the geometrical limitations discussed above (layer not covering the whole probe surface) to doubt the present water layer thickness results in dynamic conditions. Further work may be still required to definitely check the accuracy of this method. Nevertheless, as per the author's knowledge, no alternative method to measure non-intrusively thin water layers in oil-water flow with semi-dispersed flow patterns has been validated and reported so far in the literature for the sake of comparison.

Given the present experimental results, the used HF impedance probe and measurement setup provides a promising alternative way to obtain phase wetting and water layer thickness information that can then be used to check and/or develop flow models to predict fully dispersed water-in-oil flow boundaries and water wetting phenomena. This is a matter of ongoing research that will be treated in a future work. Additionally, water layer thickness data can be used to estimate

the flow rate of the segregated water and to perform better corrosion risk assessment of industrial facilities via mechanistic modelling if the chemical composition of water (pH, dissolved minerals and organics), pressure and temperature are known (Nešić, 2007; Nordsveen et al., 2003).

Due to its robustness, the actual probe design is auspicious to be used in various industrial applications:

- Flowlines, Pipelines, Risers, Manifolds:
  - Water separating from oil (or gas) can cause corrosion. Early indication of even thin layers facilitates timely measures.
  - Emulsion formation or water drop out from emulsions can be detected. Often the occurrence of emulsions is only known at inlet and outlet (or only at outlet). By detecting water layers, the probe can provide information in line.
  - Accumulation of water may impede gas flow, form slugs. Its detection allows flow control and water sweep out measures.
- Separators, Knock-out vessels:
  - Liquid collection (hydrocarbons/water). Water collecting as a free phase can cause corrosion, which might be unexpected in low water cut systems, forming thin layers.
  - Level detection allows control of bottom water level to avoid overflow.
- Storage vessels, tanks:
  - Intended for hydrocarbon storage, water may accumulate over time at bottom and cause corrosion. Detection facilitates drainage measures when needed.

Free water phase and/or water layer thickness measurements can be integrated in integrity management, which is particularly powerful if combined with multi-phase models. This would allow pro-active confirmation of model predictions in early stage; thus, reducing uncertainty and rendering management measures more robust and cost efficient. Measures could include corrosion inhibitor injection, drying, flow regime change.

#### 4. Conclusions

- A two-electrode probe of concentric design was utilized in order to measure resistance of water layers thereon using high frequency AC excitation. Moreover, theoretical expressions relating measured resistance with the water layer thickness were introduced. These showed very good agreement with experimental data obtained using calibrated water layer thicknesses.
- Phase wetting in a carbon steel pipe was successfully studied by measuring the high frequency impedance response of the two-electrode concentric probe located flush-mounted at the pipe bottom in large scale oil-dominated horizontal oil-water flow with different mixture velocities and water cut.
- The oil wet to water wet transition boundary was accurately determined via quantifying time-averaged measured impedance values.
- When determined to be in a water wet regime, it was also possible to measure *in situ* the thickness of the water layer segregated at the pipe bottom by using the introduced theory. This feature allows, for example, more comprehensive analysis of flow regimes, as well as corrosion risk assessment of industrial facilities.

#### Acknowledgments

The authors thank the following companies: BP, ConocoPhillips, Enbridge, ExxonMobil, Petronas, Total and Shell for their financial support. The valuable help from lab engineers and technicians at the Institute of Corrosion and Multiphase Technology is also greatly appreciated.

## Notation

$a$	Insulator half-width of the probe, m
$C_p$	Capacitance of the probe, F, $\Omega^{-1}.s$
$f$	Frequency of the AC excitation, Hz
$h$	Water layer thickness, m
$h^*$	Dimensionless water layer thickness
$r_i$	External radius of the inner ring electrode, m
$r_o$	Internal radius of the outer ring electrode, m
$R_s$	Resistance of the water layer, $\Omega$
$w$	Electrode width, m
$Z_p$	Impedance of the probe, $\Omega$
$Z_t$	Total measured impedance, $\Omega$
$Z_w$	Impedance of the water layer, $\Omega$

## Greek letters

$\kappa$	Water conductivity, $S.m^{-1}$ , $\Omega^{-1}.m^{-1}$
$\lambda$	Dimensionless half-distance between the end edge of each electrode, m
$\lambda_i$	Dimensionless distance between the end edge of the inner electrode and the center of the probe insulator, m
$\lambda_o$	Dimensionless distance between the end edge of the outer electrode and the center of the probe insulator, m

## References

- Al-Sarkhi, A., Sarica, C., Magrini, K., 2012. Inclination effects on wave characteristics in annular gas–liquid flows. *AIChE J.* 58 (4), 1018–1029.
- Andreussi, P., Di Donfrancesco, A., Messina, M., 1988. An impedance method for the measurement of liquid hold-up in two-phase flow. *Int. J. Multiph. Flow* 14 (6), 777–785.
- Andreussi, P., et al., 2016. Measurement of liquid film distribution in near-horizontal pipes with an array of wire probes. *Flow Meas. Instrum.* 47, 71–82.
- Asali, J.C., Hanratty, T.J., Andreussi, P., 1985. Interfacial drag and film height for vertical annular flow. *AIChE J.* 31 (6), 895–902.
- Ayello, F., et al., 2008. Determination of Phase Wetting in Oil-water Pipe Flows. NACE Corrosion 2008. NACE International, Houston TX, USA. Paper 8566.
- Ayello, F., Robbins, W., Richter, S., Nestic, S., 2013. Model compound study of the mitigative effect of crude oil on pipeline corrosion. *Corrosion* 69 (3), 286–296.
- Boyle, M.H., 1985. The electrical properties of heterogeneous mixtures containing an oriented spheroidal dispersed phase. *Colloid Polym. Sci.* 263 (1), 51–57.
- Brown, R.C., Andreussi, P., Zanelli, S., 1978. The use of wire probes for the measurement of liquid film thickness in annular gas–liquid flows. *Can. J. Chem. Eng.* 56 (6), 754–757.
- Cai, J., et al., 2012. Experimental study of water wetting in oil–water two phase flow—horizontal flow of model oil. *Chem. Eng. Sci.* 73, 334–344.
- Coney, M.W.E., 1973. The theory and application of conductance probes for the measurement of liquid film thickness in two-phase flow. *J. Phys. E Sci. Instrum.* 6 (9), 903.
- Farelas, F., Brown, B., Nestic, S., 2013. Iron Carbide and its Influence on the Formation of Protective Iron Carbonate in CO<sub>2</sub> Corrosion of Mild Steel. NACE Corrosion 2013. NACE International, Houston TX, USA. Paper 2291.
- Fried, N.A., Schiefelbein, S.L., Rhoads, K.G., Sadoway, D.R., 1993. A New Technique for Electrical Conductivity Measurements in Molten Salts. International Symposium on Molten Salt Chemistry and Technology 1993. Electrochemical Society, Pennington NJ, USA, pp. 296–305.
- Goual, L., 2009. Impedance spectroscopy of petroleum fluids at low frequency. *Energy & Fuels* 23 (4), 2090–2094.
- Hanai, T., Koizumi, N., Gotoh, R., 1962. Dielectric properties of emulsions. *Kolloid-Zeitschrift Z. für Polym.* 184 (2), 143–148.
- Judendorfer, T., Pirker, A., Muhr, M., 2011. Conductivity Measurements of Electrical Insulating Oils, IEEE 17th International Conference on Dielectric Liquids. IEEE, Trondheim, Norway. Paper 12221076.
- Kee, K.E., et al., 2015. Flow Patterns and Water Wetting in Gas-oil-water Three-phase Flow – a Flow Loop Study. NACE Corrosion 2015. NACE International, Houston TX, USA. Paper 6113.
- Kee, K.E., Richter, S., Babic, M., Nešić, S., 2016. Experimental study of oil-water flow patterns in a large diameter flow loop—the effect on water wetting and corrosion. *Corrosion* 72 (4), 569–582.
- Kermani, M.B., Morshed, A., 2003. Carbon dioxide corrosion in oil and gas production - a compendium. *Corrosion* 59 (8), 659–683.
- Koguna, A.J.A., Yeung, H., Lao, L., 2015. Study on the behaviours of settled heavier phase in two phase flows in pipelines. In: SPE Annual Technical Conference and Exhibition. SPE, Texas, USA. Paper SPE-175117-MS.
- Lotz, U., Bodegom, L.v., Ouweland, C., 1991. The effect of type of oil or gas condensate on carbonic acid corrosion. *Corrosion* 47 (8), 636–645.
- Nešić, S., 2007. Key issues related to modelling of internal corrosion of oil and gas pipelines – a review. *Corros. Sci.* 49 (12), 4308–4338.
- Nordsveen, M., Nešić, S., Nyborg, R., Stangeland, A., 2003. A mechanistic model for carbon dioxide corrosion of mild steel in the presence of protective iron carbonate Films—Part 1: theory and verification. *Corrosion* 59 (5), 443–456.
- Peng, Q., Diansheng, W., Jing, L., Yifei, C., Haotian, Z., 2014. Measurement of electrical conductivity of high insulating oil using charge decay. In: ESA Annual Meeting on Electrostatics 2014. ESA, Notre Dame IN, USA. Paper L1.
- Pots, B.F.M., Hollenberg, J.F., Hendriksen, E.L.J.A., 2006. What Are the Real Influences of Flow on Corrosion?. NACE Corrosion 2006. NACE International, Houston TX, USA. Paper 6591.
- Riaño, A.B., Bannwart, A.C., Rodriguez, O.M.H., 2015. Film thickness planar sensor in oil-water flow: prospective study. *Sens. Rev.* 35 (2), 200–209.
- Smith, S.N., Joosten, M.W., 2006. Corrosion of Carbon Steel by H<sub>2</sub>S in CO<sub>2</sub> Containing Oilfield Environments. NACE Corrosion 2006. NACE International, Houston TX, USA. Paper 6115.
- Tan, C., Li, P., Dai, W., Dong, F., 2015. Characterization of oil–water two-phase pipe flow with a combined conductivity/capacitance sensor and wavelet analysis. *Chem. Eng. Sci.* 134, 153–168.
- Tan, C., Wu, H., Dong, F., 2013. Horizontal oil–water two-phase flow measurement with information fusion of conductance ring sensor and cone meter. *Flow Meas. Instrum.* 34, 83–90.
- Tsochatzidis, N.A., Karapantsios, T.D., Kostoglou, M.V., Karabelas, A.J., 1992. A conductance probe for measuring liquid fraction in pipes and packed beds. *Int. J. Multiph. Flow* 18 (5), 653–667.
- Valle, A., 2000. CO<sub>2</sub> Corrosion and Water Distribution Two Phase Pipe Flow of Hydrocarbon Liquid and Water, NACE Corrosion 2000. NACE International, Houston TX, USA. Paper 47.
- Wu, H., Tan, C., Dong, X., Dong, F., 2015. Design of a Conductance and Capacitance Combination Sensor for water holdup measurement in oil–water two-phase flow. *Flow Meas. Instrum.* 46, Part B 218–229.
- Zhai, L.-S., Jin, N.-D., Zong, Y.-B., Hao, Q.-Y., Gao, Z.-K., 2015. Experimental flow pattern map, slippage and time–frequency representation of oil–water two-phase flow in horizontal small diameter pipes. *Int. J. Multiph. Flow* 76, 168–186.
- Zhai, L.-S., Jin, N., Zong, Y., Wang, Z., Gu, M., 2012. The development of a conductance method for measuring liquid holdup in horizontal oil–water two-phase flows. *Meas. Sci. Technol.* 23 (2), 025304.
- Zhao, Y., Markides, C.N., Matar, O.K., Hewitt, G.F., 2013. Disturbance wave development in two-phase gas–liquid upwards vertical annular flow. *Int. J. Multiph. Flow* 55, 111–129.